

# Intramolecular Microsolvation of S<sub>N</sub>2 Transition States

Stephen L. Craig and John I. Brauman\*

Contribution from the Department of Chemistry, Stanford University, Stanford, California 94305-5080

Received August 21, 1998

**Abstract:** Introduction of an  $\omega$ -substituent (CN, Cl, or OH) onto a primary  $n$ -alkyl chloride significantly enhances the rate of S<sub>N</sub>2 chloride exchange in the gas phase. Trends in reactivity suggest that the rate acceleration depends primarily on through-space solvation of the transition state, especially charge-dipole interactions. The potential energy surfaces and dynamics of these reactions are discussed.

## Introduction

Solvation plays a major role in determining rates as well as equilibria in solution ionic reactions, so that the relative thermodynamic and kinetic properties of ions in solution often do not accurately reflect the intrinsic properties of the ions themselves. The desire to understand the properties of “bare” ions has motivated the study of ion chemistry in the gas phase, where the complicating effects of bulk solvent and counterions have been removed.<sup>1</sup> Comparison of gas-phase and condensed-phase studies has facilitated a greater understanding of how ions interact with a solvating medium. The study of microsolvated reactions, in which ions are solvated by one or a few solvent molecules, has been proposed as a means of bridging the gap between the gas phase and condensed phase. Although the relationship between chemistry in microsolvated environments and chemistry in bulk solvents is not always obvious, the interactions of individual solvating groups with ionic species are fundamentally important to a wide range of chemical phenomena.

A considerable amount of work has been devoted to understanding the properties of an ion complexed to a single neutral molecule.<sup>2–14</sup> The association energies of many ion–molecule complexes have been measured with a variety of techniques, and the structures of complexes have been studied with various spectroscopies.<sup>13,15–18</sup> These studies have inves-

tigated not only the structure and energetics of ion–molecule association complexes, but also the properties of the ions and solvating molecules that determine the complexation energies and structures.

Solvation also has a dramatic influence on the rates of ionic reactions,<sup>19,20</sup> and so the effect of microsolvation on reactivity is also of interest. In the case of S<sub>N</sub>2 reactions, previous experimental<sup>21–26</sup> and theoretical<sup>27–29</sup> work has addressed the influence of a solvent molecule on S<sub>N</sub>2 potential energy surfaces. Solvation of the separated reactants and products is simply clustering of the solvent molecule to the reactant and product ion, respectively, and the thermodynamics can be determined by the usual methods. For example, in the chloride exchange reaction  $\text{Cl}^- + \text{CH}_3\text{Cl} \rightarrow \text{CH}_3\text{Cl} + \text{Cl}^-$ , a single molecule of methanol stabilizes the reactants by 17.4 kcal mol<sup>-1</sup>, the association energy of  $\text{CH}_3\text{OH}\cdot\text{Cl}^-$ .<sup>30</sup> One would also like to know the microsolvation energy of the transition state, for example,  $\text{CH}_3\text{OH}\cdot[\text{Cl}^- \cdots \text{CH}_3 \cdots \text{Cl}]^-$ , but this is much more difficult to quantify. The energetics of the transition state are usually inferred from the reaction kinetics, but the rate constants of microsolvated S<sub>N</sub>2 reactions are often very small and difficult to measure. Solvation of reactants is substantially greater than that of the transition state (Figure 1), so that upon the addition of even one solvent molecule to the ionic reactant, the transition-state energy is frequently too high for the reaction to be observed in a single-collision event, precluding accurate kinetic measure-

(1) Chabinyk, M. L.; Craig, S. L.; Regan, C. K.; Brauman, J. I. *Science* **1998**, 279, 1882–1886.

(2) Arshadi, M.; Yamdagni, R.; Kebarle, P. *J. Phys. Chem.* **1970**, 74, 1475.

(3) Kebarle, P. *Annu. Rev. Phys. Chem.* **1977**, 28, 445.

(4) Paul, G. J. C.; Kebarle, P. *J. Phys. Chem.* **1990**, 94, 5184–5189.

(5) Bartmess, J. E. *J. Am. Chem. Soc.* **1980**, 102, 2483.

(6) Caldwell, G.; Rozeboom, M. D.; Kiplinger, J. P.; Bartmess, J. E. *J. Am. Chem. Soc.* **1984**, 106, 4660–4667.

(7) Larson, J. W.; McMahon, T. B. *J. Am. Chem. Soc.* **1983**, 105, 2944.

(8) Larson, J. W.; McMahon, T. B. *J. Am. Chem. Soc.* **1984**, 106, 517–521.

(9) Larson, J. W.; McMahon, T. B. *J. Am. Chem. Soc.* **1985**, 107, 766–773.

(10) Larson, J. W.; McMahon, T. B. *J. Am. Chem. Soc.* **1987**, 109, 6230.

(11) Meot-Ner, M.; Sieck, L. W. *J. Phys. Chem.* **1986**, 90, 6687.

(12) Meot-Ner, M. M. *Acc. Chem. Res.* **1984**, 17, 186.

(13) Moylan, C. R.; Dodd, J. A.; Brauman, J. I. *Chem. Phys. Lett.* **1985**, 118, 38–39.

(14) Zhang, W.; Beglinger, C.; Stone, J. A. *J. Phys. Chem.* **1995**, 99, 11673.

(15) Mihalick, J. E.; Gatev, G. G.; Brauman, J. I. *J. Am. Chem. Soc.* **1996**, 118, 12424.

(16) Yates, B. F.; Schaefer, H. F., III; Lee, T. J.; Rice, J. E. *J. Am. Chem. Soc.* **1988**, 110, 6327.

(17) Johnson, M. S.; Kuwata, K. T.; Wong, C.-K.; Okumura, M. *Chem. Phys. Lett.* **1996**, 260, 551–557.

(18) Peiris, D. M.; Riveros, J. M.; Eyler, J. R. *Int. J. Mass. Spectrom. Ion Proc.* **1996**, 159, 169–183.

(19) Lowry, T. H.; Richardson, K. S. *Mechanism and Theory in Organic Chemistry*, 3rd ed.; Harper and Row: New York, 1987.

(20) Reichardt, C. *Solvents and Solvent Effects in Organic Chemistry*; VCH: New York, 1988; pp 129–136.

(21) Bohme, D. K.; Raksit, A. B. *J. Am. Chem. Soc.* **1984**, 106, 3447.

(22) Bohme, D. K. In *Ionic Processes in the Gas Phase*; Almoester Ferreira, M. A., Ed.; D. Reidel Publishing Co.: Dordrecht, 1984; Vol. 118.

(23) Bohme, D. K.; Raksit, A. B. *Can. J. Chem.* **1985**, 63, 3007.

(24) Henchman, M.; Hierl, P. M.; Paulson, J. F. *J. Am. Chem. Soc.* **1985**, 107, 2812.

(25) Hierl, P. M.; Ahrens, A. F.; Henchman, M.; Viggiano, A. A.; Paulson, J. F.; Clary, D. C. *J. Am. Chem. Soc.* **1986**, 108, 3142.

(26) O’Hair, R. A. J.; Davico, G. E.; Hacialoglu, J.; Dang, T. T.; DePuy, C. H.; Bierbaum, V. M. *J. Am. Chem. Soc.* **1994**, 116, 3609.

(27) Bickelhaupt, F. M.; Baerends, E. J.; Nibbering, N. M. M. *Chem. Eur. J.* **1996**, 2, 196.

(28) Tucker, S. C.; Truhlar, D. G. *J. Am. Chem. Soc.* **1990**, 112, 3347.

(29) Zhao, X. G.; Tucker, S. C.; Truhlar, G. G. *J. Am. Chem. Soc.* **1991**, 113, 826–832.

(30) Hiraoka, K.; Mizuse, S. *Chem. Phys.* **1987**, 118, 457.

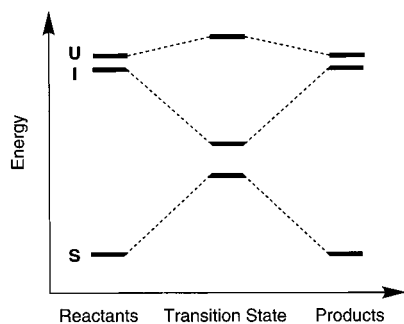


**Figure 1.** Relative potential energies of the reactants, transition states, and products of unsolvated (U), solvated (S), and intramolecularly solvated (I)  $S_N2$  chloride exchange reactions. Greater solvation of reactants typically leads to a net increase in the activation energy. In our system, intramolecular solvation stabilizes the  $S_N2$  transition state without significantly altering the energy of the reactants. The figure is not meant to convey any quantitative details about the energetics or to imply symmetry in the reaction coordinate. Intermediates and multiple transition states are omitted, and dashed lines are included for clarity.

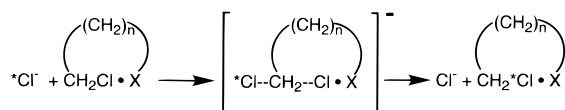


**Figure 2.** A pictorial representation of intramolecular solvation. In the reactants and products, there is negligible interaction between the chloride and solvating group S, but a strongly stabilizing interaction develops at the transition state. Note that a symmetric reaction with an unsymmetric transition state must have additional reaction paths and transition states (for example, those involving solvent transfer) which are omitted from this figure.

ments. Furthermore, competing processes in which the solvent molecule is either replaced or evaporated can complicate a kinetic analysis.

We previously reported a microsolvated gas-phase  $S_N2$  chloride exchange reaction in which the problems of preferential reactant solvation and solvent evaporation are circumvented.<sup>31</sup> In our system, the neutral reaction center (a primary alkyl chloride) is tethered to a solvating moiety by an alkyl chain (Figure 2). At large ion–neutral separation, solvation of the nucleophile (chloride ion) is negligible and the reactant energy is essentially unperturbed from the unsolvated case. At the transition state, the ion–solvent interaction increases and lowers the activation energy relative to that of the unsubstituted alkyl chlorides, resulting in  $S_N2$  rate increases of several orders of magnitude relative to those substrates. The interaction between the solvating substituent and transition state is analogous to solvation insofar as it is noncovalent and predominantly through-space rather than inductive. The observed trends in reactivity are consistent with such a mechanism, but it must be pointed out that the present systems differ substantially from traditional microsolvated reactions in that the position and also possibly the dynamics of the solvating moiety are restricted by the alkyl tether. While they are not exact mimics of a single free solvent molecule, however, the tethered solvents do provide an opportunity to examine the solvation relative to solvent position that would not be available in the usual systems.

In this work, we extend our study and discussion of these “intramolecularly solvated” reactions. All of the substrates employed have the structure  $X(\text{CH}_2)_n\text{Cl}$ , where  $n$  is the number of methylene groups separating the chloride leaving group from the solvating substituent X. For convenience, we use the abbreviated notation  $n(X)$  to refer to a molecule of formula

(31) Craig, S. L.; Brauman, J. I. *J. Am. Chem. Soc.* **1996**, *118*, 6786–7.

$X(\text{CH}_2)_n\text{Cl}$ . For example, 1,3-dichloropropane is abbreviated **3(Cl)**. The solvating moiety is varied, and corresponding changes in reactivity are observed. We quantify the solvation of the transition state by using RRKM (Rice–Ramsperger–Kassel–Marcus) theory to fit the observed rate constants, and determine the energy of the transition state relative to the separated reactants. We have also measured the complexation energy of the intermediate; it also varies with the solvating substituent, but the reactivity does not track the complexation energy, suggesting that the nature of the solvation changes as the reaction proceeds from intermediate to transition state for at least some of the substrates. Reactivity correlates strongly with the dipole moment of the solvating group, and we conclude that ion–solvent interactions such as linear hydrogen bonds and ion–induced dipole potentials, while important in determining the stability of the intermediate complex, are secondary in determining reactivity. Finally, the trends in reactivity and the results of semiempirical molecular orbital calculations suggest that, while the overall reactions are symmetrical, the intramolecular solvation of the transition states is unsymmetrical.

## Experimental Section

Experiments were conducted in an IonSpec OMEGA FTMS Fourier transform ion cyclotron resonance spectrometer (FT-ICR) equipped with a 2-in. cubic stainless steel cell and an electromagnet operating at 6.0 kG.<sup>32,33</sup> Background pressure in the vacuum chamber containing the FT-ICR cell was typically  $3 \times 10^{-9}$  Torr. All chemicals were purchased from Aldrich and subjected to multiple freeze–pump–thaw cycles prior to introduction into the vacuum chamber, as well as direct pumping of the reagents to remove volatile impurities. Reaction kinetics were independent of reagent pressure, and no chloride ion complexes with impurities were detected in the equilibrium measurements. Reagent gas pressures were measured with a Varian 844 ionization gauge, which was calibrated daily against a capacitance manometer (MKS 170 Baratron with a 315BH-1 head). Impulse excitation was used to excite the ions prior to detection. All experiments were carried out at a temperature estimated to be 350 K.<sup>34</sup>

**Reaction Kinetics.** Chloride ion was formed by electron impact ionization on  $\text{CCl}_4$ , and the less abundant  $^{37}\text{Cl}^-$  isotope was isolated with standard double-resonance ejection techniques and allowed to react with the neutral reagent. The rate of appearance of  $^{35}\text{Cl}^-$  was corrected for its natural isotopic abundance<sup>35</sup> and converted to a rate constant for  $S_N2$  chloride exchange.<sup>36</sup> Good first-order kinetics were observed for all of the reactions. Reactions were carried out across a range of neutral reagent pressures from  $3 \times 10^{-7}$  to  $2 \times 10^{-6}$  Torr, and the observed rate constants were reproducible to  $\pm 5\%$  across that range. The absolute errors in the rate constants are determined almost exclusively by the uncertainty in the absolute pressure measurements, taken to be  $\pm 30\%$ . Because much of the error in the absolute pressure measurements is likely to be systematic, the uncertainty in the relative rate constants is considerably smaller ( $\pm 10\%$ ).

**Capture Rate Constants.** The collision rate constants for ion–molecule association were calculated by using the formalism developed by Su and Chesnavich.<sup>37–40</sup> Their parametrized formula is an extension of averaged dipole orientation (ADO) theory,<sup>41</sup> and has been derived

(32) Wilbur, J. L. Ph.D., Stanford University, 1993.

(33) Zhong, M.; Brauman, J. I. *J. Am. Chem. Soc.* **1996**, *118*, 636–641.

(34) Han, C.-C.; Brauman, J. I. *J. Am. Chem. Soc.* **1989**, *111*, 6491–6496.

(35) Eyler, J. R.; Richardson, D. E. *J. Am. Chem. Soc.* **1985**, *107*, 6130.

(36) We have found no other thermodynamically allowed mechanism for the exchange of chloride ion. Elimination and anion-mediated isomerizations are both endothermic and endergonic.

(37) Chesnavich, W. J.; Su, T.; Bowers, M. T. *J. Chem. Phys.* **1980**, *72*, 2641–2655.

(38) Su, T.; Chesnavich, W. J. *J. Chem. Phys.* **1982**, *76*, 5183.

(39) Su, T. *J. Chem. Phys.* **1988**, *88*, 4102.

(40) Su, T. *J. Chem. Phys.* **1988**, *88*, 5355.

(41) Su, T.; Bowers, M. T. In *Gas-Phase Ion Chemistry*; Bowers, M. T., Ed.; Academic Press: New York, 1979; Vol. 1, pp 84–117.

empirically to reproduce the collision rates obtained from classical trajectory calculations. The Su–Chesnavich collision rate depends on the charge and mass of the ion, the polarizability, dipole moment, mass, and moments of inertia of the neutral molecule, and the temperature of the system. We obtained molecular polarizabilities from an empirical relationship.<sup>42</sup> The dipole moment and moments of inertia of each neutral molecule depend on the conformation of the alkyl chain, and all of the conformations should contribute to the collision rate. The energies, dipole moments and moments of inertia were therefore calculated for each of the stable conformations of the neutral molecules by using semiempirical molecular orbital theory with the AM1 Hamiltonian<sup>43</sup> implemented within the MOPAC<sup>44</sup> and MacSPARTAN<sup>45</sup> computational packages. A collision rate for each conformation was determined, and the total collision rate was taken to be the average of the collision rates for all conformations, weighted according to their Boltzmann distribution at 350 K. We recognize that this model is not rigorous in that it does not account properly for the conformational dynamics of the neutral molecule in the presence of an approaching ion. Nevertheless, the conformational average provides a reasonable first approximation of the ion–molecule collision rate in these systems.

**RRKM Calculations.** Activation energies were inferred from the observed rates of chloride exchange by using RRKM (Rice–Ramsperger–Kassel–Marcus) theory.<sup>46–54</sup> Recent theoretical and experimental evidence has questioned the validity of RRKM and related theories in some gas-phase  $S_N2$  reactions.<sup>55–72</sup> Nonstatistical dynamics, however, appear to be important only for ion–molecule reactions whose intermediate complexes have very short lifetimes (less than 10–100

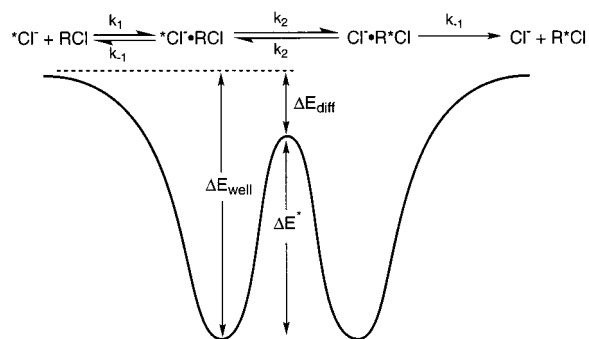


**Figure 3.** Rate constants, intermediates, and thermodynamic quantities associated with the double-well potential energy surface for  $S_N2$  chloride exchange reactions. The reaction coordinate in this figure is symmetric, but the intramolecularly solvated reactions may be unsymmetric.

### Scheme 1



ps),<sup>73–76</sup> and the intermediates of the reactions studied here should have sufficiently long lifetimes for the RRKM analysis to give accurate activation energies.

The overall kinetics of the reaction were modeled with the double-well potential energy surface shown in Figure 3. While the true minimum energy path of the reaction may not be a symmetrical double well (see Discussion, below), the model is likely to describe the kinetics of the reaction accurately. The overall rate for chloride exchange,  $k_{obs}$ , is the collision rate,  $k_1$ , multiplied by the reaction efficiency  $\Phi$ , the fraction of collisions that lead to product formation.

$$k_{obs} = k_1 \Phi \quad (1)$$

The rate constant  $k_{obs}$  may also be derived from the steady-state approximation as a function of the rate constants in Figure 3:

$$k_{obs} = \frac{k_1 k_2}{k_{-1} + 2k_2} \quad (2)$$

It then follows that  $\Phi$  is given by

$$\Phi = \frac{k_2}{k_{-1} + 2k_2}$$

and may be calculated following the  $\mu$ VTST formalism described elsewhere.<sup>73</sup> The presence of two degenerate reaction paths in the reactions of the  $\alpha,\omega$ -dichloroalkanes alters the RRKM analysis, and we have considered this effect in our calculations.

**Chloride Binding Affinities.** Chloride ion complexation energies were determined from chloride exchange equilibria between neutral substrates, Scheme 1. The equilibrium constants were determined and converted to relative free energies of chloride binding,  $\Delta G_{rel} = -RT \ln K_{eq}$ , where the temperature in the ICR is taken to be 350 K. To ensure that we were measuring the true equilibrium constant, one complex was ejected and the relative concentrations monitored with time until the steady-state ratio had been achieved. The procedure was then repeated, this time ejecting the other complex. The time for chloride exchange was increased until both experiments relaxed to the same equilibrium ratio. The measurements were repeated at multiple pressures and between various combinations of neutral substrates. As with the relative rate measurements, systematic errors in the pressure measurements cancel and the final values of  $\Delta G_{rel}$  should be accurate to within

(73) Wladkowski, B. D.; Lim, K. F.; Allen, W. D.; Brauman, J. I. *J. Am. Chem. Soc.* **1992**, *114*, 9136.

(74) Viggiano, A. A.; Morris, R. A.; Su, T.; Wladkowski, B. D.; Craig, S. L.; Zhong, M.; Brauman, J. I. *J. Am. Chem. Soc.* **1994**, *116*, 2213–2214.

(75) Craig, S. L.; Brauman, J. I. *Science* **1997**, *276*, 1536–1538.

(76) Craig, S. L.; Zhong, M.; Brauman, J. I. Submitted for publication.

(42) Miller, K. J. *J. Am. Chem. Soc.* **1990**, *112*, 8533–8542.

(43) Dewar, M. J. S.; Zoebisch, E. G.; Healy, E. F.; Stewart, J. J. P. *J. Am. Chem. Soc.* **1985**, *107*, 3902–3909.

(44) Stewart, J. J. P. *MOPAC 1990*.

(45) *MacSPARTAN*; Wavefunction, Inc.: Irvine, CA, 1996.

(46) Marcus, R. A. *J. Chem. Phys.* **1952**, *20*, 359.

(47) Marcus, R. A.; Hase, W. L.; Swamy, K. N. *J. Phys. Chem.* **1984**, *88*, 6717.

(48) Robinson, P. J.; Holbrook, K. A. *Unimolecular Reactions*; Interscience: London, 1972.

(49) Forst, W. *Theory of Unimolecular Reactions*; Academic Press: New York, 1973.

(50) Gilbert, R. G.; Smith, S. C. *Theory of Unimolecular and Recombination Reactions*; Blackwells Scientific: Oxford, 1990.

(51) Smith, S. C.; McEwan, M. J.; Gilbert, R. G. *J. Phys. Chem.* **1989**, *93*, 8142–8148.

(52) Forst, W. *J. Chim. Phys.* **1990**, *87*, 715–741.

(53) Zhu, L.; Hase, W. L. *Chem. Phys. Lett.* **1990**, *175*, 117–124.

(54) Steinfeld, J. I.; Francisco, J. S.; Hase, W. L. *Chemical Kinetics and Dynamics*; Prentice Hall: Englewood Cliffs, 1989.

(55) Basilevsky, M. V.; Ryaboy, V. M. *Chem. Phys. Lett.* **1986**, *129*, 71.

(56) Vande Linde, S. R.; Hase, W. L. *J. Am. Chem. Soc.* **1989**, *111*, 2349–2351.

(57) Vande Linde, S. R.; Hase, W. L. *J. Phys. Chem.* **1990**, *94*, 6148–6150.

(58) Vande Linde, S. R.; Hase, W. L. *J. Chem. Phys.* **1990**, *93*, 7962.

(59) VanOrden, S. L.; Pope, R. M.; Buckner, S. W. *Org. Mass. Spectrom.* **1991**, *26*, 1003.

(60) Viggiano, A. A.; Morris, R. A.; Paschkewitz, J. S.; Paulson, J. F. *J. Am. Chem. Soc.* **1992**, *114*, 10477.

(61) Graul, S. T.; Bowers, M. T. *J. Am. Chem. Soc.* **1991**, *113*, 9696–9697.

(62) Graul, S.; Bowers, M. T. *J. Am. Chem. Soc.* **1994**, *116*, 3875.

(63) Hu, W.-P.; Truhlar, D. G. *J. Am. Chem. Soc.* **1995**, *117*, 10726–10734.

(64) Hase, W. L. *Science* **1994**, *266*, 998–1002.

(65) Peslherbe, G. H.; Wang, H.; Hase, W. L. *J. Chem. Phys.* **1995**, *102*, 5626.

(66) Wang, H.; Peslherbe, G. H.; Hase, W. L. *J. Am. Chem. Soc.* **1994**, *116*, 9644.

(67) Wang, H.; Hase, W. L. *J. Am. Chem. Soc.* **1995**, *117*, 9347–9356.

(68) Wang, H.; Hase, W. L. *J. Chem. Phys.* **1996**, *212*, 247–258.

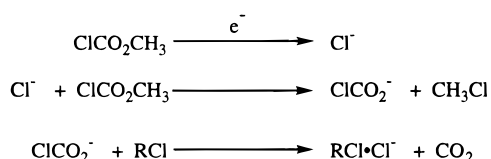
(69) Li, C.; Ross, P.; Szulejko, J. E.; McMahon, T. B. *J. Am. Chem. Soc.* **1996**, *118*, 9360–9367.

(70) Cho, Y. J.; Vande Linde, S. R.; Zhu, L.; Hase, W. L. *J. Chem. Phys.* **1992**, *96*, 8275.

(71) Craig, S. L.; Brauman, J. I. *J. Phys. Chem. A* **1997**, *101*, 4745–4752.

(72) Craig, S. L.; Zhong, M.; Brauman, J. I. *J. Am. Chem. Soc.* **1998**, *120*, 12125–12126.

## Scheme 2



0.2 kcal mol<sup>-1</sup>. Chloride-neutral complexes were formed by using the method of Larson and McMahon,<sup>77</sup> shown in Scheme 2.

Absolute chloride binding affinities were anchored to those of SO<sub>2</sub>, CF<sub>3</sub>H, and CH<sub>3</sub>CN, measured previously.<sup>77,78</sup> When necessary, the literature values were extrapolated to 350 K (the temperature of our ICR) by using the entropies of chloride binding calculated by Larson and McMahon.<sup>9,77</sup> The resulting uncertainties in the absolute free energies of chloride binding reflect uncertainties in the initial measurements as well as the errors in the entropy calculations, the uncertainty in the temperature in our instrument, and variations in our measurements. Nonetheless, good agreement is obtained between values derived from multiple reference compounds, and we estimate the error in the absolute value to be less than 1–2 kcal mol<sup>-1</sup>. Furthermore, we are interested primarily in the relative binding energies, which are independent of the reference compounds and reproducible to within 0.2 kcal mol<sup>-1</sup>.

The free energies measured in our experiments were converted to enthalpies by using entropies calculated from the vibrational frequencies obtained from semiempirical calculations.<sup>79</sup> Uncertainties in the entropy calculations arise from the vibrational frequency calculations, particularly low-frequency modes, and may be as large as a few kilocalories per mole. Because the complexes have similar structures, however, any computational error will be largely systematic, and the relative enthalpies derived from this analysis should be accurate to within 1 kcal mol<sup>-1</sup>.

**Computational Methods.** The RRKM calculations require the vibrational frequencies and rotational constants of the reactants along the dissociation path and at the  $S_N2$  transition state, and we obtained these parameters from semiempirical calculations. The energies of the  $S_N2$  intermediate complexes were determined experimentally, as described above, and combined with the molecular polarizability and conformation-averaged dipole moment to characterize the dissociation pathway using the analytical form of the potential implemented by Wladkowski, Lim, and Brauman in the RRKM program HYDRA.<sup>73,80</sup> Determination of a specific  $S_N2$  transition-state geometry was difficult, because the multidimensional potential energy surface of the reaction is very flat in the vicinity of the transition state due to low-energy internal rotations in the alkyl chains. Saddle point searches using the standard MOPAC algorithms identified multiple transition-state geometries, each characterized by an imaginary frequency for the Cl–C–Cl asymmetric stretch.

The exact geometry of the transition state is not critical to the RRKM calculations, because the only frequencies that are significantly sensitive to the precise conformation correspond to torsional degrees of freedom. At the energies of these single-collision reactions, the barriers to internal torsions are small relative to the total internal energy of the system, so we have treated the torsional degrees of freedom as free internal rotors, rather than as harmonic oscillators, for purposes of calculating the sum of states.<sup>50</sup> Barrier heights for the  $S_N2$  reactions were then calculated in the usual manner. Specifically, the activation energy in the RRKM calculations was treated as an adjustable parameter, and the value of  $\Delta E_{\text{diff}}$  that yielded the best agreement between the calculated and observed reaction efficiency was taken to be the activation energy of the reaction.

(77) Larson, J. W.; McMahon, T. B. *Can. J. Chem.* **1984**, *62*, 675–679.

(78) Hiraoka, K.; Mizuse, S.; Yamabe, S. *J. Phys. Chem.* **1988**, *92*, 3943–3952.

(79) McQuarrie, D. A. *Statistical Mechanics*; Harper and Row: New York, 1976.

(80) Wladkowski, B. D.; Lim, K. F.; Brauman, J. I. *HYDRA: Calculation of ion–molecule reaction rate coefficients using variational transition state theory*; 1991.

**Table 1.** Rate Constants, Collision Rates, and Efficiencies of the  $S_N2$  Reactions  $^*\text{Cl}^- + \text{Cl}(\text{CH}_2)_n\text{X} \rightarrow \text{Cl}^- + ^*\text{Cl}(\text{CH}_2)_n\text{X}^a$

<i>n</i>	X	<i>k</i> <sub>obs</sub> (10 <sup>-10</sup> cm <sup>3</sup> s <sup>-1</sup> )	<i>k</i> <sub>1</sub> (10 <sup>-10</sup> cm <sup>3</sup> s <sup>-1</sup> ) <sup>c</sup>	φ
1	CN	3.2 <sup>b</sup>	29	0.11
	Cl	<0.01		
2	CN	0.7	25	0.03
	Cl	<0.003		
3	OH	0.16	18	0.009
	CN	2.5	27	0.09
	Cl	0.19	19	0.01
	OH	0.19	18	0.01
	Ph	<0.01		
4	HCC	<0.01		
	CN	1.2	29	0.04
	Cl	0.10	21	0.005
5	CN	0.5	31	0.02

<sup>a</sup> Rate constants are averaged over a range of pressures (6 × 10<sup>-8</sup> to 1 × 10<sup>-6</sup> Torr) on different days. Estimated errors are ±30% in the absolute rate constants and ±10% in the relative rate constants.

<sup>b</sup> References 69 and 81. <sup>c</sup> Collision rate constant calculated according to refs 37, 39, 40, and 82 and averaged over all conformations of the neutral substrates. See text for details.

It is possible that the internal rotations required to orient the solvating dipoles to the negative charge have a sufficiently high barrier to rotation that they do not rotate freely. Such rotations are likely to be more constrained at the transition state than in the dissociation coordinate due to the increased proximity of the charge, and so the relative tightness of the  $S_N2$  transition state may be underestimated. Consequently, the  $S_N2$  barrier height derived from the RRKM analysis may overestimate the energy of the transition state, but the error that results from approximating the torsional motions as free rotors is not likely to exceed a few tenths of a kilocalorie per mole.

## Results

**Reaction Kinetics.** The rate constants of  $S_N2$  chloride exchange in a variety of  $\omega$ -substituted *n*-alkyl chlorides have been measured and are reported in Table 1. As mentioned in the Introduction, we use the abbreviated notation *n*(X) to refer to neutral substrates with the formula X(CH<sub>2</sub>)<sub>*n*</sub>Cl. We observe measurable rate constants for chloride exchange in several of the  $\omega$ -substituted alkyl chlorides (Table 1). In our previous study,<sup>31</sup> we reported that, among the nitrile-substituted alkyl chlorides,  $\gamma$ -substitution provided the greatest rate enhancement (not including  $\alpha$ -substitution). In addition to the nitrile,  $\gamma$ -substitution of a chloride or hydroxy group results in an  $S_N2$  rate constant that is large enough to be measured at the reaction times and pressures accessible in our instrument. The compounds **3**(Cl) and **3**(OH) have rate constants approximately an order of magnitude less than **3**(CN). The chloride exchange reactions of unsubstituted and alkynyl- and aryl-substituted alkyl chlorides, however, are too slow to measure.

In some cases, introduction of a substituent changes the gas-phase reactivity in a dramatically different manner than that observed in solution. For example, the  $S_N2$  chloride exchange rate constants of **3**(Cl) and CH<sub>3</sub>Cl are very similar in solution,<sup>83</sup> while we observe that the rate constant of **3**(Cl) is 3 orders of magnitude higher than that of CH<sub>3</sub>Cl in the gas phase. These reactions therefore provide another demonstration of the often dramatic differences in gas-phase and solution-phase ionic reactivity.

The influence of the length of the alkyl chain on reactivity was studied for three substituents found to increase reactivity

(81) DePuy, C. H.; Gronert, S.; Mullin, A.; Bierbaum, V. M. *J. Am. Chem. Soc.* **1990**, *112*, 8650–8655.

(82) Su, T.; Chesnavich, W. J. *J. Chem. Phys.* **1982**, *76*, 5183.

(83) Hine, J.; Ehrenson, S. J.; Brader, W. H., Jr. *J. Am. Chem. Soc.* **1956**, *78*, 2282–2284.

**Table 2.** Thermodynamic Features of the Potential Energy Surfaces of the  $S_N2$  Reactions  $Cl^- + Cl(CH_2)_nX \rightarrow Cl^- + {}^*Cl(CH_2)_nX$  (See Figure 3 for Details)<sup>a</sup>

<i>n</i>	X	$\Delta E_{well}$	$\Delta E_{well}(rel)$	$\Delta E_{diff}$	$\Delta E_{diff}(rel)$	$\Delta E^*$
1	H	-10.4 <sup>b</sup>	0	+2.5 <sup>c</sup>	0	12.9
	CN	-19.4 <sup>d</sup>	-9.0	-6.9 <sup>d</sup>	-9.4	12.5
2	H	-12.4 <sup>b</sup>	0	+3.6 <sup>e</sup>	0	16.0
	CN	-22.4	-10.0	-4.1	-7.7	18.3
	Cl	-18.6	-6.2			
	OH	-22.3	-9.9	-2.8	-6.4	19.5
3	H	-13.6 <sup>f</sup>	0	+3.1 <sup>e</sup>	0	16.7
	CN	-22.6	-8.9	-6.4	-9.5	16.2
	Cl	-19.4	-6.1	-2.5	-5.6	16.9
	OH	-22.7	-9.0	-3.0	-6.1	19.7
4	H	-14.4 <sup>f</sup>	0	+2.7 <sup>g</sup>	0	17.1
	CN	-21.7	-7.1	-4.5	-7.2	17.1
	Cl	-19.3	-4.7	-1.8	-4.5	17.5
5	H	-15.0	0			
	CN	<i>h</i>		-3.3		

<sup>a</sup> Energies in kcal mol<sup>-1</sup>. Unless otherwise noted,  $\Delta E_{well}$  is derived from chloride binding affinities from equilibrium exchange reactions, and  $\Delta E_{diff}$  is determined by using RRKM calculations to fit the experimentally observed efficiencies.  $\Delta E_{well}(rel)$  and  $\Delta E_{diff}(rel)$  are the values relative to those of the analogous unsubstituted alkyl chlorides. See text for details. <sup>b</sup> Reference 69. <sup>c</sup> Reference 84. <sup>d</sup> Reference 73. <sup>e</sup> Derived by using Marcus theory from ref 69. See text for details. <sup>f</sup> Extrapolated from values for **1**(H) and **2**(H) measured by Li et al.<sup>69</sup> and **5**(H) measured here. <sup>g</sup> Derived by using Marcus theory from Knighton et al.<sup>85</sup> See text for details. <sup>h</sup> The vapor pressure of **5**(CN) was too low to obtain reliable equilibrium binding measurements.

as  $\gamma$ -substituents: CN, Cl, and OH. In the case of OH substitution, the range of substrates is limited because **1**(OH) is not stable with respect to HCl elimination, and **4**(OH) and **5**(OH) have thermodynamically accessible ring-closing reactions that could contribute to the observed rate constant for chloride isotope exchange.

**Reaction Potential Energy Surfaces.** The salient features of the reaction potential energy surfaces for several of the reactions have been determined. From the observed kinetics, RRKM calculations are used to infer  $\Delta E_{diff}$ , the energy of the  $S_N2$  transition state relative to the separated reactants, see Figure 3. In addition, the complexation energies  $\Delta E_{well}$  of the chloride-neutral intermediates along the reaction pathway have been determined. The difference in the complexation energy and transition-state energy is the intrinsic barrier height of the reaction,  $\Delta E^*$ . The values of  $\Delta E_{diff}$ ,  $\Delta E_{well}$ , and  $\Delta E^*$  for all of the reactions studied are listed in Table 2.

It is desirable to compare the potential energy surfaces of the intramolecularly solvated reactions to those of the analogous unsubstituted alkyl chlorides. Ideally, the activation energies of the unsubstituted chloride exchange reactions would be derived from experimentally observed kinetics. Unfortunately, the  $S_N2$  reactions of  $Cl^-$  with unsubstituted RCl are very slow,<sup>84,86</sup> making accurate rate measurements difficult. For example, the rate constant of  $Cl^- + CH_3Cl$  has only recently been measured accurately by Bierbaum and co-workers<sup>84</sup> to be  $3.5 \times 10^{-14} \text{ cm}^3 \text{ s}^{-1}$ , corresponding to  $\Delta E_{diff} = +2.5 \text{ kcal mol}^{-1}$ , so it is not surprising that the rate constant for *n*-pentyl chloride ( $<10^{-12} \text{ cm}^3 \text{ s}^{-1}$ ) is too small for us to measure accurately in our system. The  $\Delta E_{diff}$  of the  $S_N2$  reactions of larger alkyl chlorides might be expected to exceed that of methyl chloride due to steric interactions at the  $S_N2$  transition state,

(84) Barlow, S. E.; Van Doren, J. M.; Bierbaum, V. M. *J. Am. Chem. Soc.* **1988**, *110*, 7240.

(85) Knighton, W. B.; Bogner, J. A.; O'Connor, P. M.; Grimsrud, E. P. *J. Am. Chem. Soc.* **1993**, *115*, 12079–12084.

(86) Van Doren, J. M.; DePuy, C. H.; Bierbaum, V. M. *J. Am. Chem. Soc.* **1989**, *93*, 1130.

but the exact values cannot be derived from experimental rate measurements.

Accurate potential energy surfaces of chloride-alkyl chloride  $S_N2$  reactions can be derived indirectly, however. Recent high-pressure mass spectrometry (HPMS) investigations by Knighton et al.<sup>85</sup> and Li et al.<sup>69</sup> have quantified the transition-state energies of a series of chloride-alkyl bromide  $S_N2$  reactions. Their studies provide a measure of the steric interactions in  $S_N2$  reactions that arise from longer alkyl chains. For example,  $\Delta E_{diff}$  for the  $S_N2$  reaction of  $Cl^- + n\text{-C}_3\text{H}_7\text{Br}$  is 1.1 kcal mol<sup>-1</sup> higher than that of  $Cl^- + \text{CH}_3\text{Br}$ . The relative activation energies for the  $Cl^- + \text{RBr}$  reactions can be converted to relative activation energies for  $Cl^- + \text{RCl}$  by using Marcus theory.<sup>87</sup> The Marcus equation has been applied previously to gas-phase  $S_N2$  reactions, and it has proven to be a quantitatively accurate means of characterizing the potential energy surfaces of these reactions.<sup>88–91</sup>

Dodd and Brauman<sup>92</sup> have redefined the Marcus equation in terms of separated reactants for ion-molecule reactions, eq 3:

$$\Delta E_{diff} = \Delta E_{diff}^0 + \frac{\Delta E_{rxn}}{2} + \frac{(\Delta E_{rxn})^2}{16(\Delta E_{diff}^0 - \Delta E_{well})} \quad (3)$$

where  $\Delta E_{diff}$  is the energy of the transition state relative to reactants,  $\Delta E_{diff}^0$  is the activation energy in the absence of a thermodynamic driving force,  $\Delta E_{rxn}$  is the endothermicity or exothermicity of the reaction, and  $\Delta E_{well}$  is the energy of the ion-molecule complex. For reactions of the form  $Cl^- + \text{RBr} \rightarrow \text{Br}^- + \text{RCl}$ ,  $\Delta E_{rxn}$  is approximately  $-8.6 \text{ kcal mol}^{-1}$ ,<sup>93</sup> and  $\Delta E_{diff}$  and  $\Delta E_{well}$  are known from the HPMS studies.  $\Delta E_{diff}^0$ , therefore, can be calculated from eq 3.

For  $S_N2$  reactions in which the nucleophile and leaving group are different, the intrinsic activation energy derived in this manner reflects the intrinsic reactivity of both the nucleophile and the leaving group. Marcus proposed in his original work<sup>87</sup> that the intrinsic component of eq 3 should be very near the mean of the activation energies of the corresponding self-reactions, in this case the two thermoneutral reactions  $Cl^- + \text{RCl}$  and  $\text{Br}^- + \text{RBr}$ .

$$\Delta E_{diff}^0 = \frac{1}{2}(\Delta E_{diff}^0(Cl, Cl) + \Delta E_{diff}^0(Br, Br)) \quad (4)$$

This validity of eq 4, known as the Marcus additivity postulate, has recently been demonstrated by Wladkowski and Brauman for some  $Cl^- + \text{RBr}$   $S_N2$  reactions.<sup>91</sup> Wladkowski and Brauman also found that  $\Delta E_{diff}^0(Br, Br)$  is 1–2 kcal mol<sup>-1</sup> lower than  $\Delta E_{diff}^0(Cl, Cl)$ , so that the activation energy of  $Cl^- + \text{RCl}$  is typically  $\sim 0.7 \text{ kcal mol}^{-1}$  greater than the value of  $\Delta E_{diff}^0$  derived from eq 3 for the  $Cl^- + \text{RBr}$  cross reaction. By using this information,  $\Delta E_{diff}$  of the symmetric  $Cl^- + \text{RCl}$  reactions was calculated from the energies reported in the earlier HPMS studies, and those values can be compared to the values of  $\Delta E_{diff}$  obtained for the  $\omega$ -substituted alkyl chlorides. The Marcus approach yields  $\Delta E_{diff} = +2.5 \text{ kcal mol}^{-1}$  for  $Cl^- +$

(87) Marcus, R. A. *Annu. Rev. Phys. Chem.* **1964**, *15*, 155–196.

(88) Pellerite, M. J.; Brauman, J. I. *J. Am. Chem. Soc.* **1980**, *102*, 5993.

(89) Pellerite, M. J.; Brauman, J. I. *J. Am. Chem. Soc.* **1983**, *105*, 2672–2680.

(90) Dodd, J. A.; Brauman, J. I. *J. Am. Chem. Soc.* **1984**, *106*, 5356–5357.

(91) Wladkowski, B. D.; Brauman, J. I. *J. Phys. Chem.* **1993**, *97*, 13158–13164.

(92) Dodd, J. A.; Brauman, J. I. *J. Phys. Chem.* **1986**, *90*, 3559.

(93) Lias, S. G.; Bartmess, J. E.; Liebman, J. F.; Holmes, J. L.; Levin, R. D.; Mallard, W. G. *Gas-Phase Ion and Neutral Thermochemistry*; 1988; Vol. 17, Supplement 1.

$\text{CH}_3\text{Cl}$ , in excellent agreement with the value inferred from the kinetics measured by Bierbaum and co-workers. The values of  $\Delta E_{\text{diff}}$  calculated for the exchange reactions of unsubstituted alkyl chlorides are reported in Table 2 along with the values derived from our experimental measurements of the intramolecularly solvated reactions.

**Transition-State Geometry.** We performed semiempirical molecular orbital calculations in an effort to locate the  $S_N2$  transition state of these reactions. The semiempirical calculations often did not define a specific  $S_N2$  transition-state geometry, because the multidimensional potential energy surface of the reaction is very flat in the vicinity of the transition state due to low-energy internal rotations in the alkyl chains. For example, depending on the starting geometries, saddle point searches with the standard MOPAC algorithms converged on several "transition-state" geometries for the reaction of  $\text{Cl}^- + \mathbf{3}(\text{CN})$ , but each is characterized by more than one imaginary frequency and is not a true transition state on the reaction potential energy surface. In each case, one of the imaginary frequencies is approximately  $490i \text{ cm}^{-1}$ , corresponding to the  $\text{Cl}-\text{C}-\text{Cl}$  asymmetric stretch, and the other is typically less than  $50i \text{ cm}^{-1}$  and corresponds to an internal torsional degree of freedom. The geometries of these "transition states" range from symmetrical (Figure 4a) to unsymmetrical (Figure 4b) and have similar energies (within  $1.0 \text{ kcal mol}^{-1}$ ).

A true transition state was found for one of the intramolecularly solvated  $S_N2$  reactions,  $\text{Cl}^- + \mathbf{2}(\text{OH})$ , and its geometry is shown in Figure 5. The transition state is characterized by a single imaginary frequency along the  $\text{Cl}-\text{C}-\text{Cl}$  asymmetric stretch, and its energy is  $1.0 \text{ kcal mol}^{-1}$  lower than that calculated for a symmetrical geometry. Furthermore, the symmetrical structure has two imaginary frequencies (corresponding to the  $\text{Cl}-\text{C}-\text{Cl}$  asymmetric stretch and rotation about the  $\text{C}-\text{C}$  bond), and is not a true transition state for the  $S_N2$  reaction at this level of theory. Previous work has shown that the calculated energetics and structures of  $S_N2$  transition states are sensitive to the level of computational theory,<sup>28,29,73,94-96</sup> and the semiempirical calculations are not definitive. Nevertheless, the calculations for  $\text{Cl}^- + \mathbf{2}(\text{OH})$  show that unsymmetrical transition-state geometries can be lower in energy than symmetrical transition states for these reactions.

## Discussion

**Background.** The results obtained in this study demonstrate that a substituent on an alkyl chain can accelerate the rate of an  $S_N2$  reaction occurring at a reaction center several bonds away. The origin of the rate enhancement does not appear to be inductive. Inductive effects would be expected to vary either monotonically with increasing alkyl chain length or perhaps in an alternating progression that decreases monotonically within sets of alternant chain lengths. The observed reactivity follows neither of these patterns. For nitrile substitution, for example, the reactivity of  $\mathbf{2}(\text{CN})$  is less than that of both  $\mathbf{3}(\text{CN})$  and  $\mathbf{4}(\text{CN})$ . The same pattern is observed between  $\mathbf{2}(\text{Cl})$ ,  $\mathbf{3}(\text{Cl})$ , and  $\mathbf{4}(\text{Cl})$ . The trends in reactivity are neither monotonic with chain length nor strictly alternating, suggesting that the origin of the rate enhancement is not inductive.

We therefore propose that the origin of the rate enhancement is primarily through-space, and as such is analogous to microsolvation of the transition state as proposed in Figure 2. Further

(94) Tucker, S. C.; Truhlar, G. G. *J. Phys. Chem.* **1989**, *93*, 8138-8142.

(95) Tucker, S. C.; Truhlar, D. G. *J. Am. Chem. Soc.* **1990**, *112*, 3338-3347.

(96) Wladkowski, B. D.; Allen, W. D.; Brauman, J. I. *J. Phys. Chem.* **1994**, *98*, 13532-13540.

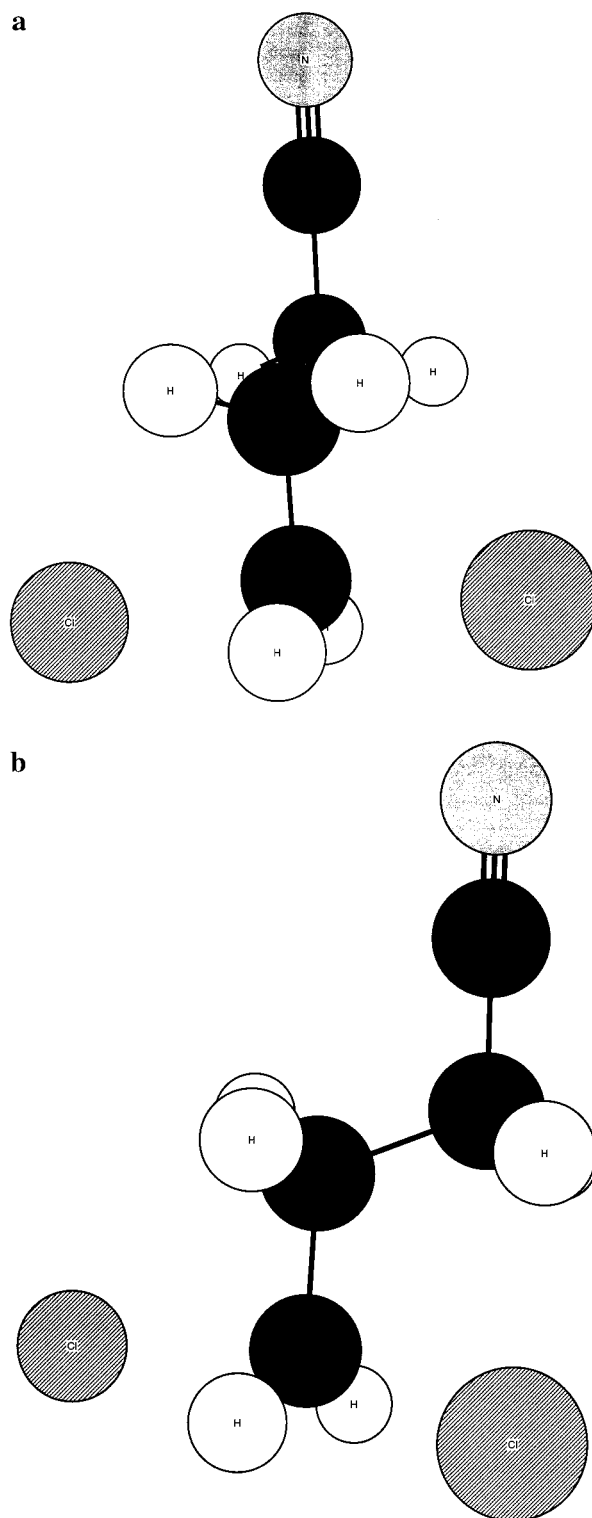


**Figure 4.** Stationary points near the transition state of the reaction of  $\text{Cl}^- + \mathbf{3}(\text{CN})$ . Each structure has two imaginary vibrational frequencies in the AM1 Hamiltonian, and is not a true transition state for the chloride exchange reaction (see text for details). The energy of the structure in part b is  $0.6 \text{ kcal mol}^{-1}$  less than that in part a at the AM1 level of computational theory.

support for the through-space model is obtained from previous condensed-phase studies by Hine and co-workers, who studied the effects of  $\beta$ - and  $\gamma$ -halogen substituents on  $S_N2$  reactivity.<sup>83,97</sup> In the condensed-phase work, through-space interactions of the substituents are significantly dampened by the presence of bulk

(97) Hine, J.; Brader, W. H., Jr. *J. Am. Chem. Soc.* **1953**, *75*, 3964.

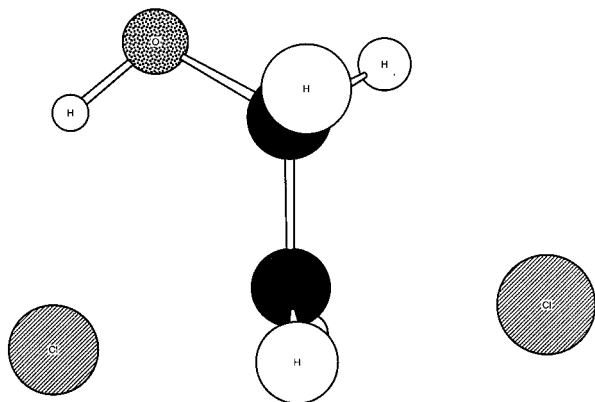


**Figure 5.** Transition state of the reaction of  $\text{Cl}^- + 2(\text{OH})$ , as calculated with use of gradient search techniques with the AM1 Hamiltonian. The unsymmetrical structure shown here is  $1.0 \text{ kcal mol}^{-1}$  lower than the symmetrical transition state at the same level of theory and, unlike the symmetrical geometry, has only one imaginary vibrational frequency.

solvent, while through-bond inductive effects are much less sensitive to the presence of the solvent. In solution, the  $\text{S}_{\text{N}}2$  reaction of **2**(Cl) is slower than that of ethyl chloride,<sup>97</sup> and the rates for **3**(Cl) and **4**(Cl) vary little from their alkyl chloride counterparts.<sup>83</sup> By comparison, we observe that, in the gas phase,  $\text{S}_{\text{N}}2$  reactions of **3**(Cl) and **4**(Cl) have transition-state energies that are 5.6 and 4.5  $\text{kcal mol}^{-1}$  lower than those of the analogous reactions of unsubstituted alkyl chlorides, respectively. The drastic difference in gas-phase and condensed-phase reactivity is consistent with the proposed model of through-space solvation of the transition state in the gas phase.

It has been previously well-documented that dipolar substituents on an alkyl chain can have a substantial influence on ionic thermochemistry, even when the substituent is several bonds away from the site of the charge. There are a variety of interactions that can contribute to the changes in thermochemistry. Mautner has summarized previous work from several laboratories that demonstrates how intramolecular noncovalent interactions can determine ionic thermochemistry in the gas phase.<sup>12</sup> For example, molecules can adopt conformations that maximize hydrogen bonding between protons and hydrogen-bond acceptors such as amines and carbonyl groups, and these interactions have a significant effect on the proton affinity of the molecule. Catalán has suggested that even unsubstituted alkyl chains adopt conformations that enhance the stability of primary alkoxy anions.<sup>98</sup> Recent work by Merrill, Dahlke, and Kass has demonstrated that the  $\beta$ -cyanoethyl carbanion is stabilized by a remarkable 29  $\text{kcal mol}^{-1}$  by the nitrile substituent.<sup>99</sup> The authors attribute the anion stability to a combination of resonance and field effects, and propose that considerable charge stabilization may be present in a range of  $\beta$ - and  $\gamma$ -substituted carbanions.

The stability of ion–molecule complexes is also enhanced by the presence of multiple solvating groups in the neutral molecule. Zhang, Beglinger, and Stone have measured the enthalpies and entropies of association of  $\alpha,\omega$ -diols with chloride anion and concluded that the diols behave as bidentate ligands for the anion.<sup>14</sup> The thermodynamic stability thus obtained is considerable; the bidentate ligand 1,4-butanediol, for example, binds chloride ion with an affinity ( $\Delta H^\circ = -30.2 \text{ kcal mol}^{-1}$ ) that is very close to the chloride binding energy of two individual ethanol molecules<sup>30</sup> ( $\Delta H^\circ = -33.7 \text{ kcal mol}^{-1}$ ). Work in the

same laboratory has also demonstrated that  $\alpha,\omega$ -diols bind protons with considerable bidentate character.<sup>100</sup> The size of the diol is important to its binding ability in each case, but the proton affinities are more sensitive to the length of the alkyl chain than are the chloride affinities.

**Binding vs Reactivity.** The charge–dipole interaction that contributes to the stability of the  $\text{S}_{\text{N}}2$  transition state should also contribute to the stability of the ion–molecule intermediate complex. Although all of the  $\omega$ -substituted alkyl chlorides demonstrate enhanced chloride binding relative to simple alkyl chlorides, stabilization of the transition state does not correlate with stabilization of the ion–molecule complex. This result stands in contrast to previous work by Wladkowski et al.,<sup>101</sup> who demonstrated that for chloride exchange reactions of substituted benzyl chlorides, reactivity correlates with the electrostatics of chloride ion complexation via a constant “intrinsic” activation barrier to nucleophilic displacement,  $\Delta E^*$ . Thus, for benzyl chlorides, the complex and the transition state are stabilized equally by a substituent on the benzene ring. In the present work, the relative stabilization of the ion–molecule complex and transition state depends on the length of the alkyl chain and the nature of the solvating group, indicating a geometric constraint to charge “solvation” at the transition state.

A good example of how geometry changes influence the relative charge stabilization of the complex and transition state in these systems is seen in **2**(OH). The ion–molecule complexation energy of **2**(OH) is quite large (22.3  $\text{kcal mol}^{-1}$ ), due in large part to a relatively strong, linear hydrogen bond between the alcohol group and chloride ion.<sup>17</sup> In the constrained geometry of the transition state, however, a linear hydrogen bond can be formed only with a severe steric penalty, and so the primary stabilization is the result of the charge–dipole interactions described above. Therefore, the complexation energy of **2**(OH) is greatly enhanced relative to **2**(H) (9.9  $\text{kcal mol}^{-1}$ ), while the transition state of **2**(OH) is stabilized relative to that of **2**(H) to a lesser extent (6.4  $\text{kcal mol}^{-1}$ ).

The differential binding of reactants and transition states is the fundamental principle underlying enzyme catalysis. The relative reactivity and chloride binding affinity of the substrates examined in this study demonstrates how the local environment surrounding a reaction site can dramatically influence ionic reactivity in the absence of bulk solvent. For example, although the ion–molecule complex of **3**(OH) is stabilized much more than its transition state relative to **3**(H), the stabilization of the ion–molecule complexes and transition states of **3**(CN) and **3**(Cl) are similar relative to the unsubstituted analogue **3**(H). As a result, **3**(CN), **3**(Cl), and **3**(H) have similar values of  $\Delta E^*$ , a few kilocalories per mole less than that of **3**(OH).

The relative stability of the complex and the transition state also depends on the length of the alkyl chain and subsequent position of the substituent. For example, the stability of the ion–molecule complexes of the nitriles relative to their unsubstituted analogues is **2**(CN) (10.0  $\text{kcal mol}^{-1}$ ) > **1**(CN) (9.0  $\text{kcal mol}^{-1}$ )  $\cong$  **3**(CN) (8.9  $\text{kcal mol}^{-1}$ ) > **4**(CN) (7.1  $\text{kcal mol}^{-1}$ ), while the transition-state stabilization is ordered **3**(CN) (9.5  $\text{kcal mol}^{-1}$ )  $\cong$  **1**(CN) (9.4  $\text{kcal mol}^{-1}$ ) > **4**(CN) (7.2  $\text{kcal mol}^{-1}$ )  $\cong$  **2**(CN) (7.7  $\text{kcal mol}^{-1}$ ). The transition state and complex stabilization do not correlate, so the stabilizing effect is partly specific to the transition state relative to the complex and reflects a geometry change between the two structures. The effect of the geometry change depends on the length of the alkyl chain. For

(98) Catalán, *J. Chem. Phys. Lett.* **1994**, 221, 68.

(99) Merrill, G. N.; Dahlke, G. D.; Kass, S. R. *J. Am. Chem. Soc.* **1996**, 118, 4462–4468.

(100) Chen, Q.-F.; Stone, J. A. *J. Phys. Chem.* **1995**, 99, 1442–1453.

(101) Wladkowski, B. D.; Wilbur, J. L.; Brauman, J. I. *J. Am. Chem. Soc.* **1994**, 116, 2471–2480.

example, the short alkyl chain in **2**(CN) precludes strong charge-dipole interactions in the transition state, but the chloride anion can be stabilized in the complex simultaneously by both the nitrile (dipole or hydrogen bond) and the dipole of the C–Cl bond.

With the addition of another methylene in **3**(CN), however, the ability of the dipole to solvate charge in the transition state increases significantly from that in **2**(CN). An important reason for this is the orientation of the C–CN dipole. The system must pay a considerable penalty in steric repulsion for the C–CN dipole in **2**(CN) to maximize its interaction with the negative charge on the Cl atoms in the transition state. In the sterically least demanding symmetrical conformation of **3**(CN), however, the C–CN dipole is oriented so that there is favorable charge-dipole interaction in the  $S_N2$  transition state. Although semi-empirical calculations suggest that the true transition state may not be symmetrical, it appears that strong charge solvation in the transition state can be achieved without severe steric repulsive interactions.

The stabilizing interaction may be quantified by comparing the  $S_N2$  activation energies of the substituted compounds to those derived from Marcus theory arguments for the unsubstituted alkyl chlorides. As reflected in the kinetics, the extent of the transition-state stabilization does not vary monotonically with the position of the substituent. For example,  $\Delta E_{\text{diff}}$  of **3**(CN) is 9.5 kcal mol<sup>-1</sup> below that of **3**(H), while  $\Delta E_{\text{diff}}$  of **2**(CN) is only 7.7 kcal mol<sup>-1</sup> below that of **2**(H). Interestingly, the transition state of Cl<sup>-</sup> + **3**(CN) is stabilized as much as the intermediate complex of that reaction, relative to the transition state and complex of the reaction Cl<sup>-</sup> + **3**(H). The added transition-state solvation of Cl<sup>-</sup> + **3**(CN), however, is still less than the chloride affinity of acetonitrile (13.4–14.4 kcal mol<sup>-1</sup>), presumably because the charge is dispersed over a greater volume in the transition state and because the orientation of the solvating moiety in **3**(CN) is somewhat restricted. Nevertheless, these results demonstrate that microsolvation of an  $S_N2$  chloride exchange transition state by acetonitrile can be substantial.

In fact, the transition-state solvation in **3**(CN) (9.5 kcal mol<sup>-1</sup>) is very similar to, and perhaps greater than, that in **1**(CN) (9.4 kcal mol<sup>-1</sup>). The charge solvation in the Cl<sup>-</sup> + **3**(CN) transition state is wholly electrostatic; resonance and orbital mixing effects should be negligible. The origin of the rate enhancement in **1**(CN) is less obvious, but previous experimental and theoretical work<sup>73</sup> in our laboratory concluded that resonance does not contribute to the reactivity observed in that system. The reactivity of **3**(CN) demonstrates that electrostatic contributions can account for the transition-state stabilization observed in **1**(CN) without a significant contribution from resonance.

**Source of Stabilization.** The task then becomes to understand what characteristics of the solvating group determine the gas-phase reactivity observed in our systems. Several solvating geometries are possible. For example, the negative charge on chloride ion is significantly solvated by acetonitrile in a geometry that includes either a linear C–H–Cl hydrogen bond or a backside ion–dipole complex,<sup>78</sup> and the energy difference between similar geometries in the ion–molecule complex of chloride ion and chloroacetonitrile is very small.<sup>73</sup> In principle, either solvating geometry could stabilize the negative charge in the  $S_N2$  transition state, and the trends in reactivity among the nitrile-substituted compounds at first seem consistent with either structure. Transition-state solvation through either a hydrogen-bonded or backside-dipole geometry would be most accessible for intermediate chain lengths, in which charge

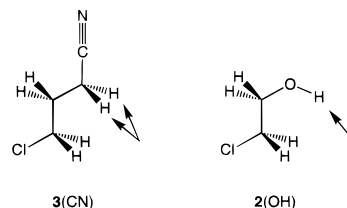


**Figure 6.** Protons capable of hydrogen bonding in **3**(CN) and **2**(OH). The proton(s) are  $\gamma$  to the chloride leaving group in each compound, so if hydrogen bonding were the primary source of charge stabilization in the  $S_N2$  chloride exchange transition state, **2**(OH) would be more reactive toward chloride exchange than **3**(CN).



**Figure 7.** The orientation of the dipole moments of acetonitrile and methanol. In acetonitrile, the molecular dipole is oriented along the C–N bond, while in methanol the dipole nearly bisects the angle formed by C–O–H.

stabilization could be achieved via formation of a structure that resembles a 5- or 6-membered ring, and the most reactive substrates **3**(CN) and **4**(CN) are the appropriate length to achieve these geometries.

A linear hydrogen-bonded geometry, however, would require that the molecule adopt a conformation with severe entropic and steric penalties, and it seems unlikely that the transition state would closely resemble such a conformation. Empirical evidence against linear hydrogen bonding in the transition state comes from the OH-substituted reagents. The alcohols should form stronger hydrogen bonds than the nitriles, as evidenced by the fact that the chloride affinity of methanol<sup>30</sup> (17.4 kcal mol<sup>-1</sup>) is higher than that of acetonitrile<sup>78,102,103</sup> (13.4–14.4 kcal mol<sup>-1</sup>), yet they are less reactive. For example, **2**(OH) and **3**(CN) have protons capable of hydrogen bonding in almost identical positions (see Figure 6), but **3**(CN) is over an order of magnitude more reactive toward chloride exchange than is **2**(OH), despite the stronger chloride–hydrogen bond interaction that is possible in **2**(OH).

Another explanation for the rate enhancement is that the transition state is stabilized by the interaction between the negative charge and the dipole along the C–X bond, rather than the electrostatic interactions associated with hydrogen bonding. If C–X dipolar interactions determine reactivity, then transition-state solvation in the series of structurally similar compounds **3**(X) should correlate with the dipole moment of the molecule CH<sub>3</sub>X. One exception to this expectation is **3**(OH). The dipole moment in methanol does not lie along the C–OH bond, but is oriented instead as shown in Figure 7. The local dipole in **3**(OH) is therefore in a similar position to that in **4**(CN), and that in **2**(OH) is similar to that of **3**(CN).

The data in Table 3 show that the calculated values of  $\Delta E_{\text{diff}}$  correlate well with the dipole moments of CH<sub>3</sub>X for the substrates **3**(X), X  $\neq$  OH, and **2**(OH). The largest dipole moment (CH<sub>3</sub>CN, 3.92 D) corresponds to the substrate with the highest reactivity. By comparison, CH<sub>3</sub>OH (1.70 D) and CH<sub>3</sub>Cl (1.87 D) have similar and smaller dipole moments, and **3**(Cl) and **2**(OH) have similar reaction rates that are less than that of **3**(CN) but still measurably faster than those of unsubstituted alkyl chlorides. Finally, nonpolar phenyl, alkynyl, and alkyl substit-

(102) Sieck, L. W. *J. Phys. Chem.* **1985**, *89*, 5552–5556.

(103) Yamdagni, R.; Kebarle, P. *J. Am. Chem. Soc.* **1972**, *94*, 2940–2943.

**Table 3.** Effect of CH<sub>3</sub>X Dipole on the Transition-State Energy of the S<sub>N</sub>2 Reaction Cl<sup>-</sup> + n(X), n(X) → X(CH<sub>2</sub>)<sub>n</sub>Cl

substrate	Δ <i>E</i> <sub>diff</sub> (kcal mol <sup>-1</sup> )	CH <sub>3</sub> X dipole (debye)
3(CN)	-6.4	3.92
2(OH)	-2.8	1.70
3(Cl)	-2.5	1.89
3(HCC)	> -1.0	0.78
3(Ph)	> -1.0	0.38
3(H)	+3.1	0.00

uents have very little polarity along the C–X bond, and the S<sub>N</sub>2 reaction of each of these substrates is over an order of magnitude less than that of 3(Cl) and below the accurate detection limit of our instrument. These data support the assertion that γ-substituents (or β-OH groups) influence gas-phase S<sub>N</sub>2 reactivity through charge-dipole interactions.

The same may not be rigorously true of longer chain lengths. Inspection of molecular models demonstrates that δ-protons can form hydrogen bonds with chlorine atoms in the S<sub>N</sub>2 transition state without the same steric penalty as γ-protons through a six-membered ring-like structure. The availability of such an interaction may explain why reactivity in 3(OH) is slightly higher than that in 2(OH), while decreased reactivity is found for 4(CN) and 4(Cl) relative to 3(CN) and 3(Cl), respectively. The observed differences in reactivity are fairly small, however, and 4(CN) is more reactive than 3(OH), so hydrogen bonding is still less important than dipolar interactions in these systems.

#### Transition State and Potential Energy Surface Symmetry.

In the most stable conformation of the reactant complex, the dipolar substituent is oriented so that solvation of the reactant chloride ion is maximized, and the product complex will adopt an analogous conformation in which the product ion is similarly solvated. To convert from one complex to the other, two processes must occur: the reactant chloride must displace the product chloride, and the solvating substituent must reorient to stabilize the charge on the product ion. We now consider whether these two events happen simultaneously or sequentially in the intramolecularly solvated reactions. Kurz and Kurz have suggested that weakly coupled motion between a solvent and solute may give rise to different time scales for reaction and solvent reorganization, and that the differences in nuclear motion will lead to a sequential mechanism.<sup>104,105</sup> Although such dynamic solvation effects may be operative in these systems, we limit our present discussion to the equilibrium structure of the transition state(s). Tucker and Truhlar have recently evaluated the contribution of nonequilibrium effects in the microhydrated reaction of chloride and methyl chloride, Cl<sup>-</sup>·(H<sub>2</sub>O)<sub>n</sub> + CH<sub>3</sub>Cl, *n* = 1, 2, and find that nonequilibrium effects have only a minor effect on the calculated rate of that reaction.<sup>28</sup>

One might expect that the dipolar field effects would be greatest in the substrates with the shortest alkyl chains, but solvation of the transition state is greater for 3(CN) and 3(Cl) than for 2(CN) and 2(Cl), respectively. One possible interpretation of the increased reactivity in the longer alkyl chains is that they may access unsymmetrical, ring-like conformations in which solvation of the transition state is enhanced. For example, structures similar to five- and six-membered rings might be invoked to explain the greater reactivity in 3(CN) and 4(CN) than in 2(CN). In this case, the solvating dipole would interact preferentially with one of the two chlorine atoms.

Symmetrical transition states cannot be easily ruled out, however. The charge solvation depends not only on the

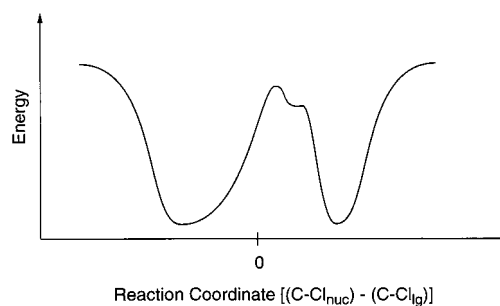


**Figure 8.** The potential energy surface along the reaction coordinate of a reaction with overall symmetry passing through an unsymmetrical transition state, such as the reaction of Cl<sup>-</sup> + 2(OH). The coordinate shown is for an intramolecularly solvated reaction in which the nucleophile is preferentially solvated in the transition state, and there may be a post-substitution intermediate with a second transition state for solvent transfer. In the event that an unsymmetrical mechanism is operative, there must exist another reaction mechanism in which the leaving group is preferentially solvated, and microscopic reversibility requires that the two pathways be equally active.

proximity of the solvent to the transition state, but also on the relative orientation of the solvating dipole with respect to the charge. Solvation is maximized when the dipolar C–X bond points directly toward the negative charge, and the Cl–C–X angle is 180°. For symmetrical transition states and C–Cl bond lengths of 2.2 Å, molecular models predict Cl–C–CN angles of approximately 103, 136, and 124° in 2(CN), 3(CN), and 4(CN), respectively. Even within a symmetrical transition state, then, the C–CN dipoles in 3(CN) and 4(CN) are more favorably oriented for charge solvation than is the dipole in 2(CN). The same is true for 3(Cl) and 4(Cl) relative to 2(Cl). Nevertheless, the S<sub>N</sub>2 transition state of any of these reactions could, in principle, be solvated more effectively if the dipole is reoriented into an unsymmetrical geometry. We therefore turn to calculations to assess whether the transition states of these reactions are symmetrical.

Semiempirical calculations show that the orientation of the solvating group influences the energy of the transition state, and although the level of theory in these calculations is not sufficient to assign a definitive transition-state geometry, the calculations demonstrate that the solvation of the transition state can be greater for unsymmetrical conformations of the alkyl chain than for symmetrical ones. For the reaction of Cl<sup>-</sup> + 2(OH), the geometry corresponding to a symmetric transition state has two negative eigenvalues associated with its force constant matrix, and an S<sub>N</sub>2 transition state of lower energy must exist. The unsymmetrical structure shown in Figure 5 is a true transition state for the S<sub>N</sub>2 reaction (one imaginary frequency of 490i cm<sup>-1</sup> in the Cl–C–Cl asymmetric stretch), and its energy is 1.0 kcal mol<sup>-1</sup> lower than the symmetric geometry at the AM1 level of theory. Differences in the charges on the chlorine atoms (-0.75 vs -0.64) and the C–Cl bond lengths (2.26 vs 2.09 Å) illustrate the unsymmetrical nature of the calculated transition state. Previous theoretical work by Chandrasekhar et al.<sup>106</sup> identified unsymmetrical transition-state structures for the S<sub>N</sub>2 reaction of Cl<sup>-</sup>·(H<sub>2</sub>O) + CH<sub>3</sub>Cl, although Tucker and Truhlar<sup>28</sup> calculated that the transition state is symmetrical and Morokuma<sup>107</sup> found transition-state structures of both types. Tucker and Truhlar<sup>28</sup> point out that such disparate results are not unexpected, given that barriers to solvent reorientation are very small. Slightly different models of solvent

(104) Kurz, J. L.; Kurz, L. C. *J. Am. Chem. Soc.* **1972**, *94*, 4451.

(105) Kurz, J. L.; Kurz, L. C. *Isr. J. Chem.* **1985**, *26*, 339.

(106) Chandrasekhar, J.; Smith, S. F.; Jorgensen, W. L. *J. Am. Chem. Soc.* **1985**, *107*, 154.

(107) Morokuma, K. *J. Am. Chem. Soc.* **1982**, *104*, 3732.

interaction, therefore, can lead to substantial qualitative differences in the transition-state structure.

If the equilibrium transition-state structure of  $Cl^- + 2(OH)$  were that shown in Figure 5, then the minimum-energy reaction path must resemble that shown in Figure 8, drawn for a reaction in which the incoming chloride ion is preferentially solvated by the dipolar substituent. The mechanism depicted in Figure 8 cannot be the lone operative reaction mechanism, however. Microscopic reversibility requires that the reverse reaction must proceed through the same transition state, and in the reverse reaction, it is the outgoing ion, rather than the incoming ion, that is preferentially solvated. Because the overall reaction is symmetric, however, the reverse reaction is identical to the forward reaction; the same reaction has two transition states that are differentiated by whether the attacking group or the leaving group experiences the greater dipolar solvation. To satisfy microscopic reversibility, the two pathways must be equally active. Half of the  $S_N2$  reactions must have solvent transfer precede chloride displacement, and in the other half solvent transfer follows chloride displacement. Similar potential energy surfaces have been observed for the calculated  $S_N2$  reactions of alkyl halides,<sup>108–110</sup> and the dynamics of such “narcissistic” reactions have been discussed previously by Salem.<sup>111–113</sup>

(108) Jensen, F. *Chem. Phys. Lett.* **1992**, *196*, 368–76.

(109) Gronert, S.; Merrill, G. N.; Kass, S. R. *J. Org. Chem.* **1995**, *60*, 488–9.

(110) Streitwieser, A.; Choy, G. S.-C.; Abu-Hasanayn, F. *J. Am. Chem. Soc.* **1997**, *119*, 5013–5019.

(111) Salem, L.; Durup, J.; Bergeron, G.; Cazes, D.; Chapuisat, X.; Kagan, H. *J. Am. Chem. Soc.* **1970**, *92*, 4472–4.

(112) Salem, L. *Acc. Chem. Res.* **1971**, *4*, 322–8.

(113) Bone, R. G. A.; Rowlands, T. W.; Handy, N. C.; Stone, A. J. *Mol. Phys.* **1991**, *72*, 33–73.

## Conclusions

Unlike the corresponding reactions in solution, the  $S_N2$  chloride exchange reactions of alkyl chlorides in the gas phase are accelerated up to several orders of magnitude when a proton on the alkyl chain is replaced with a nitrile, alcohol, or chloride moiety, even when the substituent is added several bonds away from the chloride leaving group. The trends in reactivity are consistent with a mechanism for the rate acceleration that involves through-space dipolar solvation of the ionic transition state, rather than inductive effects along the bonding framework of the molecules. The transition-state solvation effected by a  $\gamma$ -CN group is as great as that effected by an  $\alpha$ -CN group, and  $\delta$ -substitution of either a nitrile or chlorine accelerates the  $S_N2$  reaction more than in the analogous  $\beta$ -substituted substrates. The change in geometry upon going to the transition state from the ion–dipole complex causes at least some transition states to be specifically solvated relative to the bound intermediate. By using RRKM theory, the solvation of the transition state has been quantified, and the results suggest that the  $[Cl \cdots CH_3 \cdots Cl]^-$  transition state can undergo substantial microsolvation by acetonitrile (9–10 kcal mol<sup>-1</sup>) and methyl chloride (5–6 kcal mol<sup>-1</sup>). Finally, semiempirical calculations suggest that the transition states of these symmetric reactions may be unsymmetrical.

**Acknowledgment.** We thank the National Science Foundation for support of this research and a Predoctoral Fellowship (S.L.C.). S.L.C. gratefully acknowledges fellowship support from the ACS Division of Organic Chemistry (1995–96 DuPont Merck Pharmaceutical Fellowship) and Stanford University (John Stauffer Memorial Fellowship).

JA983010X